

PHASE EQUILIBRIA AND THERMODYNAMICS OF BINARY COPPER SYSTEMS WITH 3d-METALS. IV. COPPER – MANGANESE SYSTEM

M. A. Turchanin, P. G. Agraval, and A. R. Abdulov

UDC 669.35:536.717

Thermodynamic properties of alloys and phase diagram of Cu – Mn system have been assessed in the spirit of the CALPHAD-approach using simultaneously data about thermodynamic properties of phases and their equilibria. Thermodynamic data are known only for liquid and (Cu, γ Mn)-phase, model parameters for (δ Mn)- and (β Mn)-phases were therefore estimated using phase equilibria data. The excess Gibbs free energy of phases is described by models with Redlich-Kister polynomials. The models of Gibbs free energy of liquid and (Cu, γ Mn)-phase take into account excess heat capacity of these phases. Thermodynamic model of the system provides a self-consistent description of all thermodynamic values and phase equilibria, including metastable immiscibility of (Cu, γ Mn)-phase in close agreement with experimental data. Low-temperature part of the diagram is added in accordance with published data on ordering reactions in (Cu, γ Mn)-phase.

Keywords: *phase diagram, thermodynamics, thermodynamic modeling, copper based alloys, metastable transformation.*

Interaction of copper and manganese remains an object of intent attention of researchers for more than one hundred years. Initially the interest was caused by the favorable combination of mechanical and technological properties of binary alloys of the system and multicomponent compositions based on them. In addition to a good workability, manganese bronzes exhibit high-temperature strength and corrosion resistance [1]. Manganese is an effective modifying addition to cast brass, favorably affecting their technological properties [2] at the same time. To particular physical properties of the copper – manganese system it is possible to refer their high electrical resistivity [3], which not really depends on temperature, and a wide spectrum of magnetic transformations including paramagnetism, antiferromagnetism, and transition into the state of spin glasses [3, 4]. Subsequently it was established [5, 6] that alloys rich in manganese have typical combination of high strength and plasticity with very high damping capacity. These alloys effectively absorb the energy of mechanical vibration and thus may be used as construction materials in order to prevent noise and vibration [7]. The alloys rich in manganese demonstrate a reversible shape memory effect [8] that makes them promising for use as an activator material in micromachines [9].

The copper – manganese system is one of the few systems in which two transition metals differing markedly in properties demonstrate total mutual solubility. Resulting solid solution shows a tendency towards ordering in the range of copper rich alloys, and a tendency towards metastable immiscibility in the range of manganese rich alloys. All of it makes copper – manganese system an notheworthy object for study by both modern material science and fundamental investigations.

PHASE EQUILIBRIA

Stable transformations. A review of work devoted to studying the phase equilibria in the system carried out before 1939 is given in [10-12]. By the opinion of authors [10] most part of obtained results contain errors connected with the fact that manganese used in experiments contained impurities (from 2 to 10%). In [13, 14] is given a review of researches carried out before 1990 and a phase diagram for the system is suggested on the base of it.

Donbass State Mechanical Engineering Academy, Kramatorsk. Translated from Poroshkovaya Metallurgiya, Nos. 11-12(452), pp. 72-86, November-December, 2006. Original article submitted February 8, 2005.

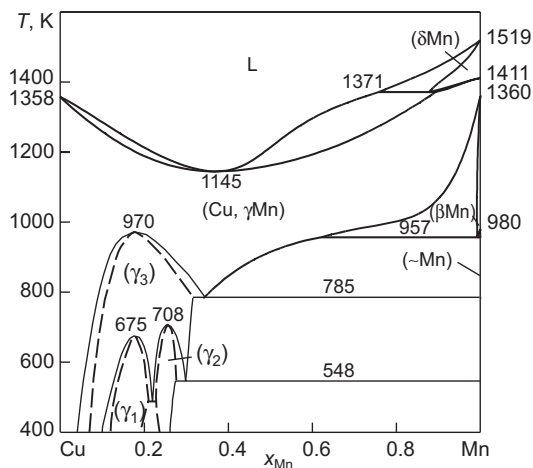


Fig. 1

Fig. 1. Phase diagram of the copper – manganese system

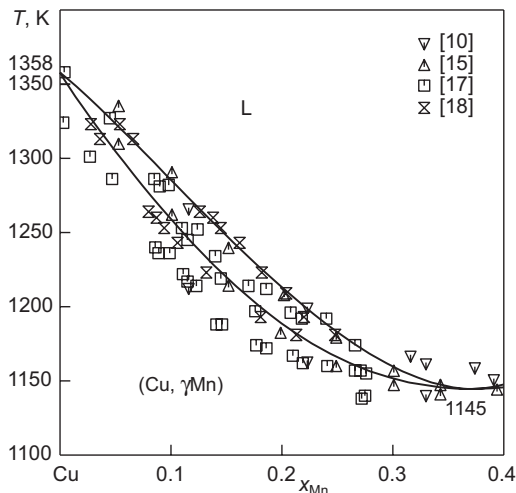


Fig. 2

Fig. 2. Experimentally established and calculated positions of the liquidus and solidus lines of the (Cu, γMn)-phase in the range of copper rich alloys

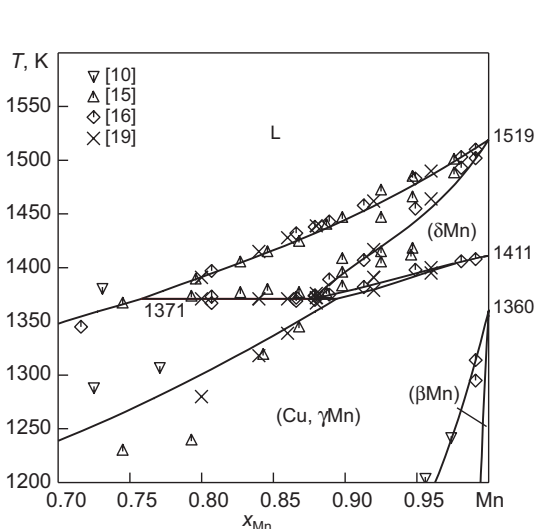


Fig. 3

Fig. 3. Experimentally established and calculated phase boundaries in the high temperature region of manganese rich alloys

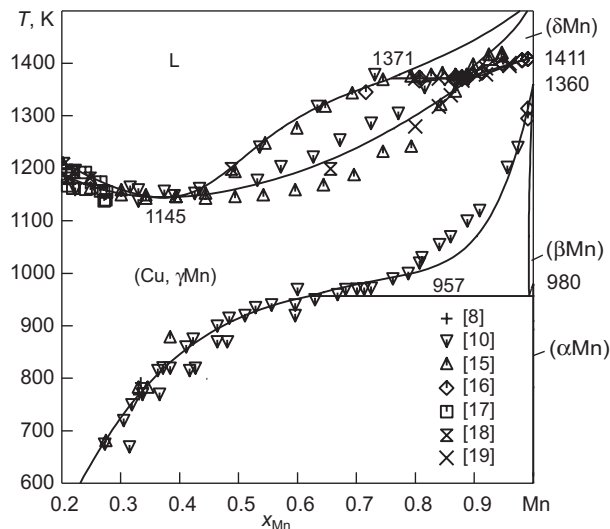


Fig. 4

Fig. 4. Experimentally established and calculated ranges for the existence of (Cu, γMn)-, (βMn)-, and (αMn)-phase

The modern ideas on phase equilibria in the system based on the results given in [10, 15-20]. Investigations were carried out by thermal [10, 15-17], metallographic and x-ray [10, 17], electronmicroprobe [18] analyses, and also by use of electrical resistance [15, 17-20], magnetic susceptibility [19], hardness [17] and thermal expansion [20] measurements of alloys.

As follows from Fig. 1, there are two regions of primary solidification in the system: (Cu, γMn) and (δMn), whose boundaries were studied in [10, 15-19]. Solid solutions (Cu, γMn), (δMn) and liquid (L) participate in the catatctic reaction $(\delta\text{Mn}) \Leftrightarrow \text{L} + (\text{Cu}, \gamma\text{Mn})$. The liquidus line of the system has a minimum.

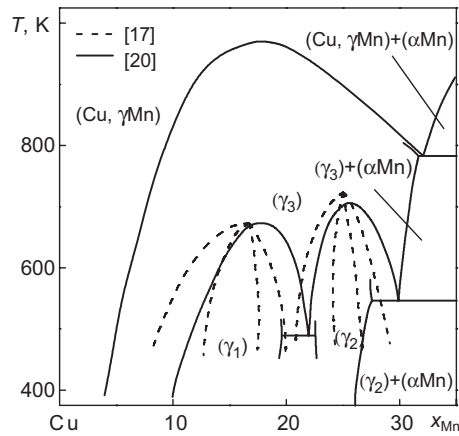


Fig. 5. Experimentally established boundaries for the regions of ordering in (Cu, γ Mn)-phase

Transformations in the solid phase are connected with polymorphism of manganese and ordering processes in (Cu, γ Mn). Boundaries of existence of equilibrium (Cu, γ Mn)-phase were studied in [10, 15, 16, 20]. Results of works [10, 15] for the phase boundary (Cu, γ Mn)/((α Mn) + (Cu, γ Mn)) are in principal agreement. In the case of the (Cu, γ Mn)/((β Mn) + (Cu, γ Mn)) boundary the phase line obtained in [15] appears 100-200 K higher than the results of work [10] to which later was given preference.

According to the review given in [13, 14] the solubility of copper in (α Mn) and (β Mn) is insignificant and it does not exceed tenths of a percentage. At the same time this conclusion appears to be in contradiction with the data [10] in which it was established, that transformation with participation of (α Mn) and (β Mn) phases occurs between 953 and 963 K, whereas for the corresponding polymorphic transformation in pure manganese a temperature of 978 K was obtained. Such reduction in temperature may be connected with eutectoid transformation (β Mn) \leftrightarrow (Cu, γ Mn) + (α Mn), and its value, comprising ~ 20 K, points to the possibility of dissolution of copper in (β Mn). In favor of this suggestion point results of work [16] where the temperature range of existence of two-phase region ((β Mn) + (Cu, γ Mn)) was established for alloy with $x_{\text{Mn}} = 0.99$. There are no experimental data pointing to the solubility of copper in (α Mn). The results of experimental studies of phase equilibria are presented in Figs. 2-4.

By differential thermal analysis, hardness and microstructure study of annealed and quenched alloys, x-ray analysis and measurement of electric resistance at the high-temperature region it was established in [17] that in (Cu, γ Mn) alloys rich in copper there are transformations in the solid state connected with ordering and formation of the compounds $\text{Cu}_5\text{Mn} - (\gamma_1)$ and $\text{Cu}_3\text{Mn} - (\gamma_2)$. This part of the phase diagram was studied in details in [20-22] by dilatometry, electric resistance and elasticity modulus measurements. In [21] formation of (γ_1) and (γ_2) phases was confirmed. In [20, 22] along with this fact the formation of a high-temperature modification of the compound $\text{Cu}_5\text{Mn} - (\gamma_3)$ was established. This phase takes part in the eutectoid transformation with (α Mn): (Cu, γ Mn) \leftrightarrow (γ_3) + (α Mn). With the temperature lowering the high-temperature modification of Cu_5Mn undergoes eutectoid decomposition (γ_3) \leftrightarrow (γ_1) + (γ_2) with formation of its low-temperature modification (γ_1) and the ordered structure (γ_2). The (γ_2) phase is in equilibrium with (α Mn) and participates in the eutectoid reaction (γ_3) \leftrightarrow (γ_2) + (α Mn). Presented in [17, 20] boundaries of existence of ordered structures and phase equilibria with them are given in Fig. 5.

Parameters of invariant equilibria obtained by different authors are presented in Table 1.

Metastable transformations. The possibility of metastable transformations connected with participation of supercooled (Cu, γ Mn)-phase is being discussed in modern literature. In alloys with a manganese content $x_{\text{Mn}} > 0.4$ during tempering at 673-873 K there is metastable separation of FCC-solution (Cu, γ Mn) into isomorphic high disperse FCC-phases (Cu, γ Mn)₁ and (Cu, γ Mn)₂, accordingly depleted and enriched in manganese, existing for a long time [5].

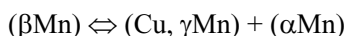
This metastable separation significantly precedes the separation from (Cu, γ Mn) of equilibrium phase (α Mn) in time. Boundaries of immiscibility limits were studied by hardness measuring [23], neutron diffraction and x-ray methods [5].

TABLE 1. Experimentally Determined and Computed Parameters of Equilibrium Invariant Transformations in the Copper – Manganese System
 $(\delta\text{Mn}) \Leftrightarrow (\text{Cu}, \gamma\text{Mn}) + \text{L}$

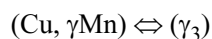
T, K	x_{Mn}^{L}	$x_{\text{Mn}}^{(\delta\text{Mn})}$	$x_{\text{Mn}}^{(\text{Cu}, \gamma\text{Mn})}$	Source
1388	0.780	0.885	0.895	Experiment [15]
1371	0.760	0.875	0.882	Experiment [16]
1371	0.770	0.875	0.882	Experiment [19]
1371	0.758	0.878	0.894	Results of calculations*



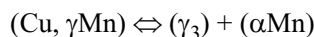
T, K	x_{Mn}^{L}	Source
1143	0.384	Experiment[10]
1143	0.394	Experiment [15]
1145	0.370	Results of calculations



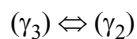
T, K	$x_{\text{Mn}}^{(\beta\text{Mn})}$	$x_{\text{Mn}}^{(\text{Cu}, \gamma\text{Mn})}$	$x_{\text{Mn}}^{(\alpha\text{Mn})}$	Source
953-963	-	-	-	Experiment [10]
957	0.993	0.621	1.000	Results of calculations



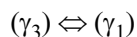
T, K	$x_{\text{Mn}}^{(\text{Cu}, \gamma\text{Mn})}$	Source
970	0.177	Experiment [20]



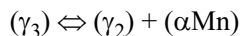
T, K	$x_{\text{Mn}}^{(\text{Cu}, \gamma\text{Mn})}$	$x_{\text{Mn}}^{(\gamma_3)}$	$x_{\text{Mn}}^{(\alpha\text{Mn})}$	Source
785	0.330	0.310	1.000	Experiment [20]



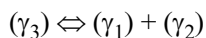
T, K	$x_{\text{Mn}}^{(\gamma_3)}$	Source
723	0.250	Experiment [17]
708	0.256	Experiment [20]



T, K	$x_{\text{Mn}}^{(\gamma_3)}$	Source
673	0.163	Experiment [17]
675	0.177	Experiment [20]



T, K	$x_{\text{Mn}}^{(\gamma_3)}$	$x_{\text{Mn}}^{(\gamma_2)}$	$x_{\text{Mn}}^{(\alpha\text{Mn})}$	Source
548	0.293	0.270	1.000	Experiment [20]



T, K	$x_{\text{Mn}}^{(\gamma_3)}$	$x_{\text{Mn}}^{(\gamma_1)}$	$x_{\text{Mn}}^{(\gamma_2)}$	Source
488	0.215	0.198	0.225	Experiment [20]

* Present work's data.

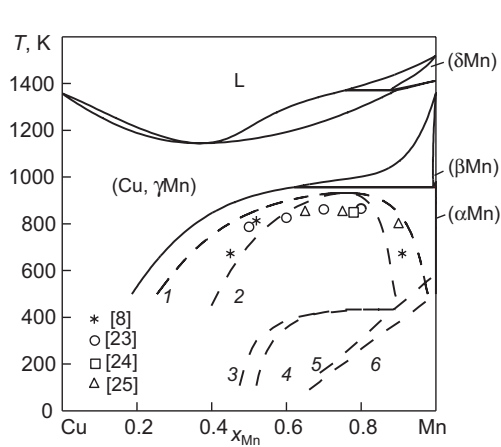


Fig. 6

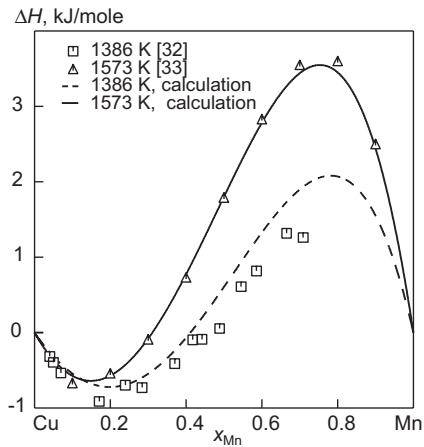


Fig. 7

Fig. 6. Calculated phase diagram of the copper – manganese system and its metastable continuation for (Cu, γMn)-phase: 1) binodal of (Cu, γMn)-phase; 2) spinodal of the (Cu, γMn)-phase; 3, 4) temperature and concentration limits of the transformation (Cu, γMn) ⇌ (Cu, γMn)' [8]; 5, 6) temperature and concentration limits of the transformation (Cu, γMn)₁ + (Cu, γMn)₂ ⇌ (Cu, γMn)' [8]

Fig. 7. Experimentally established and calculated integral mixing enthalpies of liquid copper and manganese

The authors of [23] report that done conclusions were verified by the results of measurements in a DSC according to which separation of (Cu, γMn) is accompanied by an exothermic heat effects. Results of earlier investigations [24, 25] are also summarized in work [23].

On quenching from the (Cu, γMn) region there is a low-temperature diffusionless martensitic transformation accompanied by formation of a (Cu, γMn)' phase with a FCT-lattice [5, 8, 9, 23] in alloys with a high concentration of manganese. This transformation provides the development of a reverse shape memory effect, has magnetic nature and is caused by antiferromagnetic ordering of the magnetic moments of manganese atoms. The heat treatment regime for the (Cu, γMn)-phase noticeably affects on the parameters of the martensitic transformation. The temperature of (Cu, γMn) ⇌ (Cu, γMn)' transformation is close to room temperature for alloys with $x_{Mn} = 0.8$ and rises with an increase of manganese concentration. Separation of (Cu, γMn) during preliminary tempering leads to an increase in temperature and expansion of concentration region of the corresponding martensitic transformation (Cu, γMn)₁ + (Cu, γMn)₂ ⇌ (Cu, γMn)' [8, 9]. In [9] martensitic transformation in alloy with $x_{Mn} = 0.86$ was studied by measuring electric resistance and DSC. The results of investigations of metastable transformations in the copper – manganese system are presented in Fig. 6.

Alloys of (Cu, γMn)-phase demonstrate magnetic properties that essentially depend on concentration, temperature, and heat treatment regime [4, 26-28]. In [14] a magnetic phase diagram of (Cu, γMn) is presented. It was constructed on the basis of consistent information obtained in [4, 29-31].

THERMODYNAMIC PROPERTIES OF PHASES

Thermodynamic properties of liquid alloys. Mixing enthalpies in (Cu – Mn) system was studied with help of calorimetric methods in [32-34]. In [32] investigations were carried out at 1386 K in the composition range $x_{Mn} = 0-0.71$ (Fig. 7). The value of the first mixing enthalpy of manganese was determined to be close to -9 kJ/mole. Fourteen values of the mixing enthalpy were obtained in [32] and alternating-sign character of this function was established. The minimum of integral enthalpy of mixing -0.8 kJ/mole was found to be close to $x_{Mn} = 0.2$. The maximum ΔH was not established by experiment. Obtained values were described by the following equation

$$\Delta H = x_{Mn}(1-x_{Mn})(-9.16+17.78x_{Mn}-6.07x_{Mn}^2) \text{ kJ/mole.}$$

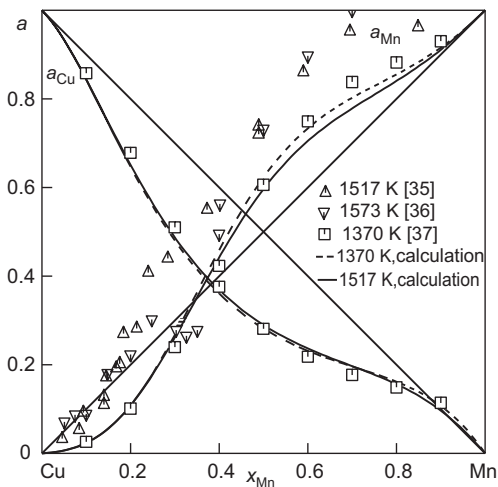


Fig. 8

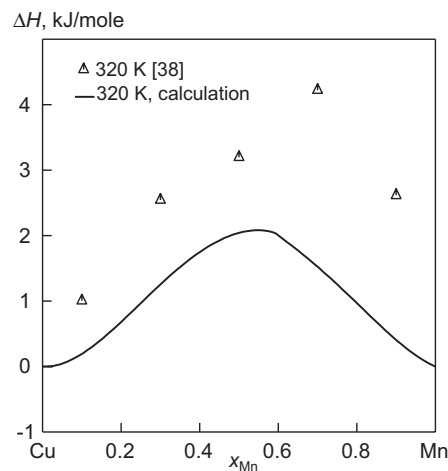


Fig. 9

Fig. 8. Experimental and calculated thermodynamic activities of components of melts for copper – manganese system

Fig. 9. Experimental and calculated mixing enthalpies of copper and manganese in (Cu, γ Mn)-phase

In [33, 34] formation enthalpy of liquid copper – manganese alloys was studied over the whole concentration range at 1573 K for 150 compositions. Integral mixing enthalpy of manganese with copper over the whole concentration range was described by the expression

$$\Delta H = x_{\text{Mn}}(1 - x_{\text{Mn}})(-17.55 + 162.40x_{\text{Mn}} - 682.75x_{\text{Mn}}^2 + 1618.73x_{\text{Mn}}^3 - 2008.58x_{\text{Mn}}^4 + 1370.87x_{\text{Mn}}^5 - 413.38x_{\text{Mn}}^6) \text{ kJ/mole.}$$

Integral mixing enthalpy has variable sign: negative in the compositions range $x_{\text{Mn}} = 0-0.3$ and positive in $x_{\text{Mn}} = 0.3-1$. The minimum coordinates of integral mixing enthalpy are -0.6 ± 0.2 kJ/mole and $x_{\text{Mn}} = 0.10$, and the maximum 3.6 ± 0.4 kJ/mole and $x_{\text{Mn}} = 0.75$ (Fig. 7). The first mixing enthalpy of manganese is -17.5 ± 5.1 kJ/mole. Dissolution of the first copper samples in manganese was accompanied by significant endothermic effect: 29.6 ± 4.0 kJ/mole. Satisfactory agreement should be noted for results obtained in [33] at temperature 1573 K with the data in [32], which demonstrate lower endothermic values over a wide compositions range at temperature of 1386 K.

The activities of components of liquid alloys for Cu – Mn system (Fig. 8) were studied by authors in [35-37].

In [35] the manganese activity was studied by the Knudsen effusion method for 18 alloys within the temperature range $T = 1278-1596$ K and compositions range $x_{\text{Mn}} = 0.048-0.850$. According to data [35] the activity isotherm of manganese at 1517 K is presented in Fig. 8. The activity of manganese demonstrates strong positive deviation from ideality in the compositions range rich in manganese and negative deviations in alloys rich in copper. The most intensive change of a_{Mn} is observed close to $x_{\text{Mn}} = 0.18$.

In [36] the manganese activity was studied for 14 alloys by touch instant emf method at 1573 K in the compositions range $x_{\text{Mn}} = 0.051-0.700$. These results do not conflict with the data of [35], but they are characterized by a great values scattering.

In [37] the activities of copper and manganese were studied by the mass-spectrometric Knudsen effusion method for 12 alloys with $x_{\text{Mn}} = 0.053-0.759$ at temperature 1370 K. In Fig. 8 activities isotherms of copper and manganese calculated from a model of excess Gibbs free energy of melts are presented:

$$\Delta G^{\text{exc}} = x_{\text{Mn}}(1 - x_{\text{Mn}})(72444.4 + 7.6474T + (5186.58 - 22.9183T)x_{\text{Mn}} + (18928.4 + 15.3798T)x_{\text{Mn}}^2) \text{ J/mole.}$$

Minimum excess free energy $\Delta G_{\text{min}}^{\text{exc}} = -3.31$ kJ/mole was established at $x_{\text{Mn}} = 0.28$ in [37].

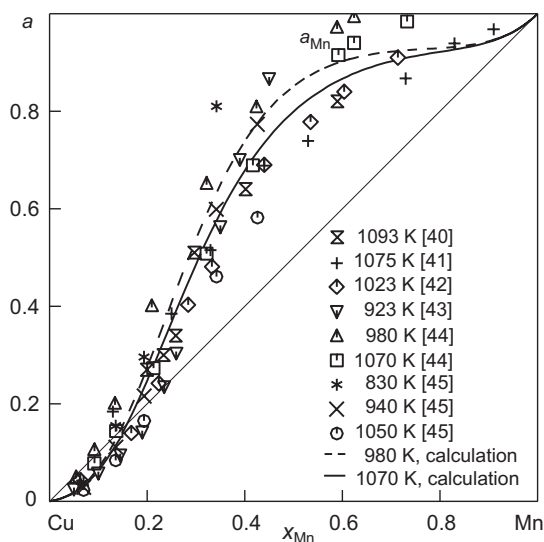


Fig. 10

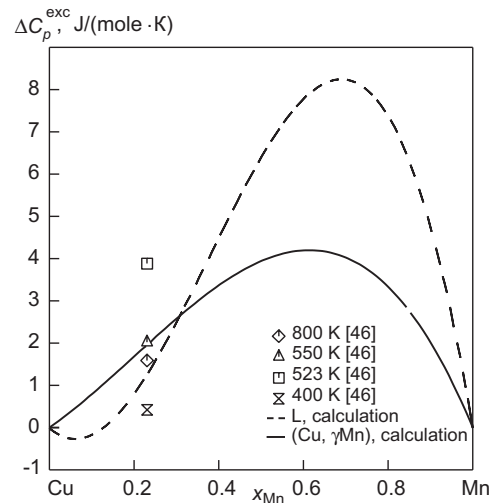


Fig. 11

Fig. 10. Experimental and calculated thermodynamic activities of manganese in (Cu, γ Mn)-phase: for manganese pure (γ Mn) is taken as the standard state

Fig. 11. Experimental and calculated excess heat capacity of (Cu, γ Mn)-phase and calculated excess heat capacity of melts of the system

According to experimental data, activities of copper and manganese in liquid alloys, as well as the enthalpy of mixing, has an alternating-sign nature: they become negative in the compositions range rich in copper, and negative in the range rich in manganese.

Thermodynamic properties of solid alloys. Currently only thermodynamic properties of (Cu, γ Mn)-phase have been experimentally studied. In [38] the formation enthalpy of solid alloys was investigated by the calorimetric method of dissolution in tin. Small endothermic values reaching 4.2 kJ/mole at a maximum with $x_{\text{Mn}} = 0.8$ were obtained for isotherms of formation enthalpy at 320 K. Mixing enthalpy of components in (Cu, γ Mn)-phase (Fig. 9) was given on the basis of these experimental data in [14].

Thermodynamic activity of manganese was studied by the Knudsen effusion method in [39-41]. In [40] a_{Mn} isotherm was obtained at 1093 K on the basis of measuring the vapor pressure of manganese for six alloys with $x_{\text{Mn}} = 0.20-0.59$ in the temperature range 1091-1119 K. In [39] thermodynamic properties are studied in the temperature range 1163-1211 K for alloys with $x_{\text{Mn}} = 0.1-0.95$, and the manganese activity was determined at 1163 and 1211 K. Unfortunately results of this work over a wide compositions range relate to the solid-liquid state and they cannot be directly compared with the data of other authors. In [41] thermodynamic properties were investigated in the temperature range 973-1273 K for eight alloys with $x_{\text{Mn}} = 0.13-0.91$, and a manganese activity isotherm is presented at 1075 K. In [42, 43] thermodynamic activity of manganese was studied by the emf method with salt electrolyte. Ten alloys of copper with manganese at $x_{\text{Mn}} = 0.06-0.82$ were examined in the range 930-1100 K, and a_{Mn} isotherm was found at 1023 K. In [43] investigations were performed for nine alloys rich in copper ($x_{\text{Mn}} = 0.050-0.450$) in the temperature range 750-1075 K. The emf method with solid CaF_2 electrolyte was used to study thermodynamic properties of alloys in later works [44, 45]. In [44] investigations were performed within the range of 950-1070 K for eight alloys with $x_{\text{Mn}} = 0.055-0.727$. As a result of it two isotherms of manganese activity at 980 and 1070 K were obtained. In [45] in the range 744-1108 K and concentration range $x_{\text{Mn}} = 0.070-0.426$ a_{Mn} isotherms at 830, 940, and 1050 K were obtained as a result of studying the properties of six alloys.

Results of the cited above works are presented in Fig. 10. All of the values of manganese activity are given relative to the standard state of (γ Mn). As follows from figure in the region of copper rich alloys the manganese activity demonstrates small negative or zero deviations from ideality. With an increase of manganese concentration there is an increase in the positive deviation from ideality. Essential scatter of experimental data of different authors is typical, even in those cases when investigations were performed using similar methods at comparable temperature ranges.

In [46] the temperature dependence of heat capacity of alloy with $x_{\text{Mn}} = 0.231$ was investigated using a high-temperature adiabatic calorimeter within the temperature range of 293-823 K. In [47] the heat capacity of seven alloys with $x_{\text{Mn}} = 0.278-0.900$ was investigated in the temperature range 720-1120 K, and the following empirical equation was obtained

$$C_p = 25.31 + 0.0106T - (8.47 - 0.00833T)x_{\text{Mn}} \text{ J/(mole} \cdot \text{K)}.$$

In [48] the heat capacity of antiferromagnetic phase was studied in the region of manganese rich alloys. In spite of the fact that works, devoted to investigation of the heat capacity are quite fragmentary, they point to positive values of excess heat capacity of (Cu, γ Mn)-phase (Fig. 11).

OTHERMODYNAMIC ASSESSMENT OF THE SYSTEM AND THE MODEL

Versions of copper – manganese phase diagram were presented in [37, 45, 49] as a result of thermodynamic evaluations of the system. In [49] the data on phase equilibria [12, 50] and thermodynamic properties of phases [51] were used for analytical description of the system. Thus, the majority of experimental thermodynamic information obtained for liquid alloys wasn't taken into account for receiving models [49]. Therefore the thermodynamic evaluation of the system, which was presented in the work allows to describe observed phase transformations qualitatively up to the metastable separation of (Cu, γ Mn)-phase, but quantitative agreement with the experimental data is not observed neither for the phase boundaries nor for thermodynamic values (except for (Cu, γ Mn)-phase).

Parameters of thermodynamic models of liquid, (Cu, γ Mn) and (δ Mn)-phases were presented in [45], what made it possible to describe correctly the liquidus and solidus lines of the system, but led to erroneous results for the formation enthalpy of melts and the solubility limits of (Cu, γ Mn)-phase.

Thermodynamic description of the system obtained in [37] agrees qualitatively with the known experimental thermodynamic dataset. However, it is impossible to reproduce the phase diagram as a whole with the presented in that work coefficients of models and it's connected with the overestimation of the thermodynamic stability of (δ Mn)-phase at temperatures below 1300 K.

Thus, the imperfection of the known attempts to implement a thermodynamic evaluations of the copper – manganese system can be related to the absence of complete description of experimental data on thermodynamic properties of phases and phase equilibria. The most difficultly reproducible part of the phase diagram is the solubility line of (Cu, γ Mn)-phase. Its complex concentration path wasn't reproduced in any of the known works above. Another unclear point of phase equilibria in the system remains the solubility of copper in (α Mn) and (β Mn) that wasn't experimentally studied and didn't become a subject of theoretical modeling. From the viewpoint of thermodynamics the question of excess heat capacity of phases remains almost completely not examined, whereas for (Cu, γ Mn)-phase there is direct experimental evidence of non zero values of this property, and for melts of the system a similar conclusion may be drawn on the basis of analyzing the temperature dependence of the integral mixing enthalpy.

Thermodynamic evaluation of the system was performed within the framework of the CALPHAD method in the present work. The dependence of Gibbs free energy for the ϕ phase on temperature and concentration was described by the expression

$$G^\phi = (1 - x_{\text{Mn}})(G_{\text{Cu}}^\phi - H_{\text{Cu}}^{\text{SER}}) + x_{\text{Mn}}(G_{\text{Mn}}^\phi - H_{\text{Mn}}^{\text{SER}}) + RT((1 - x_{\text{Mn}})\ln(1 - x_{\text{Mn}}) + x_{\text{Mn}}\ln x_{\text{Mn}}) + \Delta G_{\text{exc}}^\phi(x_{\text{Mn}}, T),$$

where $(G_{\text{Cu}}^\phi - H_{\text{Cu}}^{\text{SER}})$ and $(G_{\text{Mn}}^\phi - H_{\text{Mn}}^{\text{SER}})$ are energies of pure copper and manganese; $\Delta G_{\text{exc}}^\phi(x_{\text{Mn}}, T)$ is the excess Gibbs free energy. The data for thermodynamic properties of copper and manganese were taken from the SGTE database [52]. In order to describe the thermodynamic properties of copper in a isomorphous state (β Mn) we used the expression

$$({}^{\circ}G_{\text{Cu}}^{\text{CUB}-\text{Al3}} - H_{\text{Cu}}^{\text{SER}}) = ({}^{\circ}G_{\text{Cu}}^{\text{FCC}-\text{Al}} - H_{\text{Cu}}^{\text{SER}}) + 2218 \text{ J/mole},$$

which was accepted in accordance with [49].

In order to describe the excess term of Gibbs free energy of solid and liquid solutions the next expression was used

$$\Delta G_{\text{exc}}^{\phi}(x_{\text{Mn}}, T) = (1 - x_{\text{Mn}})x_{\text{Mn}} \sum_{i=0}^n (1 - 2x_{\text{Mn}})^i (A_i + B_i T + C_i T \ln(T)),$$

where i is the power of the Redlich-Kister polynomial; A_i , B_i , C_i are coefficients of the model.

On choosing the model for this or that phase we were guided by the following considerations. At first the qualitative information about the nature of the temperature and concentration dependences of excess thermodynamic properties of each of the phases should be accounted and the mathematical model should be selected, that makes it possible to get a correct description of the known thermodynamic information. In the course of further calculation of model parameters within the framework of the CALPHAD method not only the value of the considered coefficients should be established, but also the adequacy of the model should be analyzed on the basis of determining the possibility to describe a set of thermodynamic properties and phase transformations in the system within its framework.

The most valid preliminary conclusions about the required set of coefficients we have made for models of thermodynamic properties of liquid alloys and (Cu, γ Mn)-phase. In both cases studied thermodynamic functions are characterized by complex concentration paths with variable sign, the temperature dependence, and there is direct or indirect evidence on difference from zero and a complex concentration path of the excess heat capacity of these phases. Therefore for these phases we adopted the following set of coefficients in the first stage of the calculations: A_0 , B_0 , C_0 , A_1 , B_1 , C_1 , A_2 , B_2 . For (δ Mn)-phase, which has an extended temperature and concentration range of existence, the following set of coefficients was adopted: A_0 , B_0 , A_1 , B_1 . In the case of (β Mn)-phase only the regularity parameter A_0 was accepted. Dissolution of copper in (α Mn)-phase was out of our consideration. The basis for this was the fact, that there wasn't any indications in modern literature on the change of lattice parameter for (α Mn)-phase, which was formed in course of ageing of supercooled (Cu, γ Mn)-phase solutions. It should be noted that in the cited above works [5, 8, 25]

TABLE 2. Optimized Parameters of Thermodynamic Models for the Phases L, (δ Mn), (Cu, γ Mn), and (β Mn) Phases of the Copper – Manganese System

$\Delta G_{\text{exc}} = (1 - x_{\text{Mn}})x_{\text{Mn}} \sum_{i=0}^n (1 - 2x_{\text{Mn}})^i (A_i + B_i T + C_i T \ln(T))$				
i	A_i		B_i	C_i
L				
0	-33031.98		202.95	-25.6
1	32943.75		-284.65	34.26
2	4992.56		-7.71	-
(δ Mn)				
0	35975.16		-23.27	-
1	5529.64		4.6	-
2	21473.05		-	-
(Cu, γ Mn)				
0	-202.6		117.13	-16.2
1	1507.25		-76.136	9.03
2	-5716.55		1.9	-
3	-		-3.88	-
(β Mn)				
0	30000		-	-

the corresponding process was studied by precise highly sensitive methods. Modeling of transformations connected with the low-temperature ordering of (Cu, γ Mn)-phase was not performed.

Model parameters were optimized with using “Thermo-Calc” program. The data on thermodynamic properties of phases and available information on parameters of invariant transformations were used at the first stage of thermodynamic optimization. Even at this stage it was established that the results of study of thermodynamic activity of copper [35, 36] doesn't correspond to the data [37] and results of calorimetric works [32, 33]. Still the attempts to take them into account lead to a thermodynamic model pointing to the possibility of separation in the liquid phase. Subsequently the data [35, 36] were excluded from optimization. At the second optimization stage experimental data on the position of phase boundaries of stable transformations and the position of the metastable binodal for (Cu, γ Mn)-phase were included. The structure of models for the thermodynamic properties of phases was clarified. The coefficient B_3 was added to the model for (Cu, γ Mn)-phase making it possible to improve the configuration of its solubility lines and the position of this line in relation to the binodal, and the coefficient A_2 was added for (δ Mn)-phase that made it possible to clarify the coordinates of the reaction $\delta\text{Mn} \Leftrightarrow (\text{Cu}, \gamma\text{Mn}) + \text{L}$ and interphase boundaries for (δ Mn), (Cu, γ Mn).

Obtained model parameters are presented in Table 2. Phase equilibria in this system and the thermodynamics of its phases can be described by a set of 23 coefficients. It should be noted that this number of coefficients twice as much those sets presented for this system in [37, 49]. At the same time exactly in this case it was possible for the first time to achieve not only qualitative, but also quantitative agreement between known thermodynamic values and the parameters of phase equilibria.

RESULTS OF CALCULATIONS AND DISCUSSION

Thermodynamic properties. As follows from Figs. 7 and 8, the proposed model for the liquid phase makes it possible to describe experimental values of thermodynamic properties of the melts [32, 33, 37] with satisfactory accuracy. Calculated in this work values of excess heat capacity of melts are presented in Fig. 11. This function is alternating-sign, as well as thermodynamic activities of components and their mixing enthalpy. Its value is close to zero or negative in the region of copper rich alloys, and positive in the region of manganese rich alloys, reaching a maximum of 8 J/(mole · K) close to $x_{\text{Mn}} = 0.7$.

Satisfactory description may also be achieved for thermodynamic properties of (Cu, γ Mn)-phase. Isotherms for the thermodynamic activity of copper calculated at 980 and 1070 K are presented in Fig. 10. The best agreement for calculated values may be noted for the data in [44], and the isotherm of properties obtained in [45] at 940 K. In Fig. 9 the calculated isotherm is demonstrated for the integral mixing enthalpy of FCC-solutions and the corresponding values obtained in [38]. As follows from Fig. 9, the values we have obtained appear to be less endothermic, but taking into account the error of calorimetric procedure the satisfactory agreement is observed with experimental data. The excess heat capacity of the FCC-solution is positive (Fig. 11), and reaches the maximum value of 4.2 J/(mole · K) at $x_{\text{Mn}} = 0.6$.

According to the carried out calculation, thermodynamic properties of (δ Mn) and (β Mn) in the region of their existence is characterized by positive deviations from ideality.

Phase equilibria. As follows from Figs. 2-4 and Table 1, satisfactory description for phase equilibria of the system was achieved in the present work. In the region of copper rich alloys calculated liquidus and solidus lines and the results of work [18] agree best of all with each other. For manganese rich alloys the calculated phase boundaries for liquid average experimental values obtained in [15, 16, 19] for (δ Mn) and in [10, 15, 18, 19] for (Cu, γ Mn).

Solubility line calculated for (Cu, γ Mn)-phase (Fig. 4) reflect all features of this interphase boundary established in [10, 15, 20]. Features of modeling of this phase boundary should be considered along with questions about the metastable separation of FCC-solution and the solubility of copper in (β Mn) and (α Mn). Supplementary calculations have shown, that in order to improve the conformity between results of calculations and experimental values for this interphase boundary at $x_{\text{Mn}} = 0.8-0.9$, where the error of the description reaches 40 K, it is necessary to assume a solubility of ~1.2 at.% Cu in (β Mn) simultaneously with solubility of ~0.7 at.% Cu in (α Mn) by retaining the temperature of the eutectoid transformation within the limits 953-963 K [10]. We do not accept this version since it is

not confirmed by the data of x-ray and neutron diffraction investigations of phases. Adopted in the present work parameters of the model lead to a terminal solubility of copper in (β Mn) equal to 0.7 at.%, that entirely agrees with the value estimated in [13, 14] by the data of x-ray investigations.

It follows from Fig. 6 that the calculated binodal for (Cu, γ Mn)-phase passes 50-80 K above the corresponding experimental values, and it has a maximum of 932 K with $x_{\text{Mn}} = 0.76$. All attempts to improve the agreement between calculation and experiment for this metastable equilibrium showed that it can be achieved only under simultaneous worsening of solubility description for the (Cu, γ Mn)-phase. At the same time the corresponding phase boundary of stable transformation passes below a set of experimental points. An indication of the possible reason for this unavoidable divergence between experiment and calculation for the boundary of metastable (Cu, γ Mn)-phase separation is given in [5, 23]. In both cited above works, devoted to studying temperature and concentration limits for the immiscibility region, conclusions were made on the basis of studying different physical properties of alloys obtained by quenching from the region of existence equilibrium of FCC-solution and then annealed at the temperature of interest. The authors in [5, 23] indicate that there are the development of very fine two phase structure in alloys quenched at 1073-1090 K, which are connected with the predominance in lattice pairs of similar atoms. This conclusion was made on the basis of studying the structure of samples by neutron diffraction and electron microscopy. It indicates that the temperature for the start of separation may be higher than that detected by different physical methods, whose sensitivity is sufficient for observing the process of separation only in macroscopic areas of the alloy. In this case the binodal, that in the present work was obtained as a result of optimizing of more than 100 experimental points for phase equilibria and thermodynamic properties of (Cu, γ Mn)-phase, seems to be a reliable theoretical result.

The modeling of transformations connected with ordering in the (Cu, γ Mn)-phase was not performed in the present work. The indications on these transformation are taken from consistent results of [17, 20]. Calculated solubility line of (Cu, γ Mn)-phase close to $x_{\text{Mn}} = 0.3$ demonstrate a good description of corresponding phase boundary established in [20]. It allowed us to connect the part of the phase diagram calculated in the present work and that studied in [20]. Result of this synthesis is presented in Fig. 1, where bold lines show phase boundaries calculated within the framework of the present thermodynamic evaluation of the system, fine lines include the results obtained in [20], and broken lines are the schematic position of boundaries, whose existence arise from the Gibbs phase rule. Suggested phase diagram does not contradict the main set of those experimental results, which are known currently for the thermodynamics and phase equilibria of the system. Additional studies directed towards clarifying phase boundaries and thermodynamic parameters of transformations in this region are necessary for theoretical description of ordering in FCC-solution.

REFERENCES

1. O. M. Byalik, V. S. Chernenko, V. M. Pisarenko, and Yu. N. Moskalenko, *Metallurgy: Textbook, in 2 Vols., reprinted and amended* [in Ukrainian], Politekhnik, Kiev (2002).
2. V. M. Vozdvizhenskii, V. A. Grachev and V. V. Spasskii, *Cast Alloys and Their Melting Technology in Engineering: Teaching Textbook for Engineering Schools* [in Russian], Mashinostroenie, Moscow (1984).
3. *Properties of Elements: Handbook* [in Russian], M. E. Drits (ed.), Metallurgiya, Moscow (1985).
4. P. Gibbs, T. M. Harders, and J. H. Smith, "The magnetic phase diagram of CuMn," *J. Phys. F. Met. Phys.*, **15**, 213-223 (1985).
5. E. Z. Vintaikin, D. F. Litvin, and V. A. Udovenko, "Fine crystalline structure in high damping copper – manganese alloys," *Fiz. Metall. Metallovedenie*, **37**, No. 6, 1228-1237 (1974).
6. S. Laddha and D. C. Van Aken, "On the application of magnetomechanical models to explain damping in an antiferromagnetic copper-manganese alloy," *Met. Mater. Trans.*, **26A**, 957-964 (1995).
7. K. Sugimoto, T. Mori, and S. Shiode, "Effect of composition on the internal friction and Young's modulus in γ -phase Mn – Cu alloys," *Metal Sci. J.*, **7**, 103-108 (1973).
8. E. Z. Vintaikin and G. I. Nosova, "Reversible shape memory effect in alloys of the Mn – Cu system," *Metall. Term. Obrab. Metallov*, No. 9, 34-37 (1996).
9. K. Tsuchiya, H. Sado, S. Edo, et al., "Effect of ageing on martensitic transformation in gamma-MnCu alloy," *Mater. Sci. Eng.*, **285A**, 353-356 (2000).

10. R. S. Dean, J. R. Long, T. R. Graham, et al., "The copper – manganese equilibrium system," *Trans. ASM*, **34**, 443-464 (1945).
11. N. N. Ivanov-Skoblikov, "Modern state of studying and constructing the phase diagram for the copper – manganese – aluminum system," *Zap. Leningrad. Gorn. Inst.*, **29**, No. 3, 152-180 (1954).
12. M. Hansen and K. Anderko, *Structure of Binary Alloys, Vol. 2* [Russian translation], Metallurgiya, Moscow (1962).
13. N. A. Gokcen, "The Cu – Mn (Copper – Manganese) System," *J. Phase Equilib.*, **14**, No. 1, 76-83 (1993).
14. N. A. Gokcen, "Cu – Mn (Copper – Manganese)," in: Phase Diagrams of Binary Copper Alloys, ASM International, Ohio, USA (1994).
15. G. Grube, E. Oestreicher, and O. Winkler, "The copper – manganese system," *Z. Elektrochem.*, **45**, 776-784 (1939).
16. A. Hellawell and W. Hume-Rothery, "The constitution of alloys of iron and manganese with transition elements of the first long period," *Philos. Trans. R. Soc. (London)*, **249A**, 417-459 (1957).
17. E. M. Sokolovskaya, A. T. Grigor'ev, and E. M. Smirnova, "Transformations in the solid state in alloys of the copper – manganese system rich in copper," *Zhurn. Neorg. Khim.*, **7**, No. 11, 2636-2638 (1962).
18. E. Schurmann and E. Schultz, "Untersuchungen zum Verlauf der Liquidus und Soliduslinien in den Systemen Kupfer – Mangan und Kupfer – Nickel," *Z. Metallkunde*, **62**, No. 10, 758-762 (1971).
19. E. Wachtel, P. Terzieff, and J. Bahle, "Construction and magnetic properties of manganese-rich copper-manganese and manganese-tin alloys," *Monatsch. Chem.* **117**, No. 12, 1349-1366 (1986).
20. T. Gödecke, "Physikalische Messungen an Kupfer – Mangan – Legierungen. III. Einfluss der Abschrecktemperatur auf den elektrischen Widerstand und die Dilatation der Legierungen," *Z. Metallkunde*, **81**, 826-835 (1990).
21. W. Köster and T. Gödecke, "Physikalische Messungen an Kupfer – Mangan – Legierungen. I. Die Ordnungsumwandlungen im Bereich der gamma-Phase des Systems," *Z. Metallkunde*, **80**, 761-765 (1989).
22. T. Gödecke and W. Köster, "Physikalische Messungen an Kupfer – Mangan – Legierungen. II. Zustandsänderungen beim Anlassen der von 850°C abgeschreckten Legierungen," *Z. Metallkunde*, **80**, 766-773 (1989).
23. J. M. Vitek and H. Warlimont, "On a metastable miscibility gap in gamma – manganese – copper alloys and the origin of their high damping capacity," *Met. Sci.*, **10**, No. 1, 7-13 (1976).
24. H. J. Stokes and I. D. Harwin, "The effect of aging on Young's modulus, electrical resistivity and hardness of 80 : 20 manganese – copper alloy," *J. Inst. Met.*, **89**, 77-79 (1960).
25. J. H. Smith and E. R. Vance, "Decomposition of γ -phase manganese – copper alloys," *J. Appl. Phys.*, **40**, No. 12, 4853-4858 (1969).
26. P. A. Beck, "Some recent results on magnetism in alloys," *Met. Trans.* **2**, 2015-2024 (1971).
27. P. A. Beck, "Comments on micromagnetism," *J. Less-Common Met.*, **28**, 193-199 (1987).
28. D. Chowdhury, T. M. Harders, A. Mookerjee, and P. Gibbs, "Theoretical justification of the magnetic phase diagram of Cu – Mn alloys," *Solid State Comm.*, **57**, No. 2, 603-605 (1986).
29. G. E. Bacon, I. W. Dunmur, J. H. Smith, and R. Street, "The antiferromagnetism of manganese – copper alloys," *Proc. Roy. Soc. (London), A*, **241**, 223-228 (1957).
30. J. E. Zimmerman, A. Arrott, H. Sato, and S. Shinozaki, "Antiferromagnetic transition in γ -phase Mn-alloys," *J. Appl. Phys.*, **35**, No. 3, 942-943 (1964).
31. G. E. Bacon and N. Cownam, "A study of some alloys of γ -manganese by neutron diffraction," *J. Phys. C. Solid State Phys.*, **3**, No. 3, 675-686 (1970).
32. S. Sato and O. J. Kleppa, "Thermochemistry of liquid alloys of transition metals. I. The systems Mn – Cu and Mn – Sn," *Met. Trans.*, **10B**, 63-66 (1979).
33. M. A. Turchanin, A. V. Kokhan, and S. V. Porokhnya, "Calorimetric study of thermodynamic properties of manganese – copper alloys," *Rasplavy*, No. 3, 17-19 (1994).

34. M. A. Turchanin and I. V. Nikolaenko, "Enthalpies of formation of liquid (copper + manganese) alloys," *Met. Mater. Trans.*, **28B**, No. 3, 473-478 (1997).
35. P. J. Spencer and J. N. Pratt, "Thermodynamic study of liquid manganese – copper alloys," *Trans. Faraday Soc.*, **64**, No. 6, 1470-1476 (1968).
36. K. Okajima and H. Sakao, "Activity measurements of the binary Mn-base alloys by the TIE method," *Trans. J. Inst. Met.*, **16**, No. 2, 87-93 (1975).
37. J. Vrest'al, J. Stepankova, and P. Broz, "Thermodynamics of manganese – copper system. Knudsen-cell spectrometric study of the liquid Cu – Mn system and calculation of the phase diagram," *Scand. J. Met.*, **25**, No. 5, 224-231 (1996).
38. J. N. Pratt and A. W. Bryant, "Thermodynamics of alloys. Calorimetric studies of manganese – copper and palladium – aluminum alloys," *US Clearing House Fed. Sci. Techn. Inform.*, No. 705, 644 (1969).
39. G. V. Evseeva and A. M. Evseev, "Thermodynamic properties of alloys of the manganese – copper system," *Zhurn. Fiz. Khim.*, **37**, No. 6, 1411-1412 (1963).
40. B. F. Peters and D. R. Wiles, "A vapor study of the alloys of manganese with copper," *Canad. J. Chem.*, **41**, No. 10, 2591-2599 (1963).
41. R. W. Krenzer and M. J. Pool, "Thermodynamic properties of copper – manganese alloys," *Trans. Met. Soc. AIME*, **245**, 91-98 (1969).
42. V. N. Eremenko, G. M. Lukashenko, and V. R. Sidorko, "Thermodynamic properties of alloys of manganese with transition elements of the fourth period (Cr, Fe, Co, Ni) and with copper," *Russ. J. Phys. Chem.*, **42**, 343-346 (1968).
43. A. F. Alabyshev, M. V. Kamenetskii, M. V. Morachevskii, and V. A. Petrov, "Study of thermodynamic properties of the manganese – copper system by an emf method," *Elektrokhimiya*, **6**, No. 11, 1709-1710 (1970).
44. J. P. Hajra, "Thermodynamics of copper – manganese alloys," *Scr. Met.*, **13**, No. 3, 173-175 (1979).
45. K. Lewin, D. Sichen, and S. Seetharaman, "Thermodynamic study of the Cu – Mn system," *Scand. J. Met.*, **22**, No. 6, 310-316 (1993).
46. E. Scheil and W. Normann, "Investigation of the short-range order formation in a copper – manganese alloy with an adiabatic high-temperature calorimeter," *Z. Metallkunde*, **51**, 165-171 (1960).
47. B. F. Naylor, "Heat contents above 25°C of seven manganese – copper alloys," *Bur. Mines RI*, 3835-3848 (1946).
48. K. Hirano, H. Maniva, and Y. Takagi, "Specific heat of antiferromagnetic phase in Mn-rich Cu – Mn binary alloys," *Acta Met.*, **6**, 64 (1958).
49. L. Kaufman, "Coupled phase diagrams and thermochemical data for transition metal binary systems – III," *CALPHAD*, **2**, No. 2, 117-146 (1978).
50. D. T. Hawkins and R. Hultgren, *Metals Handbook, Vol. 8*, ASM, Metals Park, Ohio (1973).
51. R. Hultgren, et al., *Selected Values of the Thermodynamic Properties of Binary Alloys*, ASM International, Metals Park, Ohio (1973).
52. A. T. Dinsdale, "SGTE data for pure elements," *CALPHAD*, **15**, No. 4, 317 (1991).